# Stability of Oil-in-Water Emulsions Containing Proteins

Ivan B. Ivanov,* Elka S. Basheva,* Theodor D. Gurkov,* Assen D. Hadjiiski,* Luben N. Arnaudov,* Nikolina D. Vassileva,* Slavka S. Tcholakova,* and Bruce E. Campbell[†]

*Laboratory of Chemical Physics Engineering,[‡] University of Sofia, Faculty of Chemistry, James Bourchier Avenue 1, Sofia 1164, Bulgaria

[†]Kraft Foods, Inc., Technology Center, 801 Waukegan Road, Glenview, Illinois 60025, USA

E-mail for correspondence: Ivan.Ivanov@LTPH.BOL.BG

[‡]Formerly: Laboratory of Thermodynamics and Physico-Chemical Hydrodynamics

**ABSTRACT**

This work is focused on the mechanisms for stabilisation of oil-in-water emulsion drops pressed against a homophase. With increasing concentration of a globular protein (β-lactoglobulin) in the aqueous continuous phase the drop stability is improved considerably. Repulsive interactions (other than electrostatics) prevent rupture of the intervening o/w/o films at elevated concentrations. Then, the critical disjoining pressure for coalescence is higher than the equilibrium disjoining pressure which is established when the drop arrives at the surface. The latter fact correlates with very long lifetimes of drops. Conversely, at low concentrations (below ~$10^{-3}$ wt%) the films rupture soon after the process of thinning is completed. Faster formation of saturated adsorption layers is probably responsible for the more efficient stabilisation with rising concentration. The adsorption kinetics in the time scales of seconds and minutes is rather sensitive to the protein content. Interfacial rheological measurements give evidence that with increasing concentration of protein the layer is mechanically reinforced to some extent.

# 1 INTRODUCTION

Our aim in this work is to perform model investigations on the stabilising role of increasing concentration of surface-active agent (protein) in O/W emulsions. We are interested especially in relatively low concentrations (before saturation of the interface), because the latter case is relevant to emulsification in real systems. Indeed, just after new droplets are formed the coverage $\Gamma$ of the o/w surfaces has to increase, starting virtually from zero. This process takes time, during which coalescence is most probable [1]. Hence, in the initial moments one has to consider stability under conditions of incomplete adsorption, $\Gamma<\Gamma_{eq}$. Here $\Gamma_{eq}$ refers to equilibrium at the specified bulk concentration, according to the adsorption isotherm. During emulsification drops are formed, collide, and may recoalesce for a fraction of a second [1], [2]. Under these conditions of renewing surface the adsorbed amount, $\Gamma$, does not succeed to reach saturation and stays low, $\Gamma<\Gamma_{eq}$. The kinetic value $\Gamma$ would correspond to a hypothetical equilibrium at a certain lower concentration than that which is actually present in the bulk of the emulsified system. That is why we choose to study low concentrations.

It is a common truth that more surfactant provides better stability of the drops against coalescence. However, there might be different reasons for this effect. First, one can mention the role of the surface mobility for the rate of thinning of the films which intervene between approaching (deformable) drops [3]. With slower thinning more time is allowed for emulsifier adsorption and formation of compact layers. The thinning rate of films whose interfaces are mobile can exceed several times the respective rate in the case of full immobility. The Gibbs elasticity of the liquid boundary and the surface diffusivity of surfactant species were shown to be responsible in determining the thinning behaviour [3].

Second, the interfacial rheology (viscosity and elasticity) has been recognised to be an important factor for preventing film rupture through the mechanism of growing fluctuation waves. Adsorbed viscoelastic layers are very efficient in damping the surface corrugations [4], which will otherwise lead to drop coalescence. The role of the surface viscosity for the hydrodynamic behaviour (thinning and rupture) of foam films has been investigated thoroughly by Ivanov & Dimitrov [5], [3]. Third, the interactions between the film surfaces are greatly influenced by the adsorbed amphiphilic molecules. Repulsive forces may arise from electrostatics (when the surfactant-laden liquid boundaries are charged), from steric, oscillatory structural, hydration, protrusion interactions [6], etc. All these forces tend to prevent the film interfaces from coming into direct contact, thus suppressing the rupture.

Here we shall be concerned with food proteins, and in particular, with the main globular protein from whey- β-lactoglobulin (BLG). A major difference between the low

molecular weight surfactants and the proteins is the ability of the latter to form an entangled gel-like network, multilayers or lumps on the o/w interface. This leads to peculiarities in the manifestation of the governing factors for stability. Below we will discuss data for the coalescence stability of emulsion droplets in connection with experimental results from different model investigations: adsorption kinetics, interfacial rheology, disjoining pressure in thin films, measured as a function of the thickness, critical pressure for film rupture. It will be demonstrated that the augmented stability of the drops at increased concentration of protein correlates with faster adsorption and concomitant higher threshold pressures for film rupture. Reinforced surface rheology is also a consequence of the increased protein content, but this effect is less relevant to stability because the interfaces are tangentially immobile even at the lowest concentration studied. Thus, the hydrodynamics of the thinning films turns out to be unimportant in the case of protein.

## 2 EXPERIMENTS

### 2.1 Materials

Beta-lactoglobulin from bovine milk was purchased from Sigma Co. (L-0130, mixture of A and B variants). As oil phases in the emulsions we used xylene and soybean oil (commercial products). They were additionally purified by passing through a column filled with the chromatographic adsorbent Florisil-F101. Approximately 10 g of adsorbent were needed for each 50 ml of oil. The oil was kept in closed bottles in a dark dry place.

Aqueous phase was prepared using water purified by a Millipore Milli-Q unit (resistance 18.2 $M\Omega.cm^{-1}$ ). The ionic strength was adjusted to 0.15 M with NaCl (Merck), preliminarily baked for 5 hours at 450ºC in order to remove all organic contaminants. We worked at two values of pH: "natural" (without additives for regulation), which is about 6.2 for BLG solutions, and the isoelectric point, pH=5.2. When pH=5.2 was desired, the acidity was maintained by citrate buffer whose total concentration was 0.12 M; 0.03 M NaCl were also added in that case.

### 2.2 Methods

**2.2.1. Drops against an interface.** The lifetime of oil drops pressed by buoyancy to a large homophase (i.e., to a flat oil/water boundary) was measured. The drops were released from a glass capillary immersed in the aqueous phase. The experimental method is described in details in Ref. [7]. We applied two different modes of operation: (i) oil drops were formed at the capillary tip and were detached immediately. Thus, the drop surface was fresh; (ii) initially, a crude O/W emulsion was prepared by hand-shaking. After some ageing

time (more than 15 minutes) the glass capillary was filled with the emulsion and oil droplets were ejected toward the O/W interface.

**2.2.2. Interfacial tension.** We applied du Nouy platinum ring method to measure the tension of the oil/water boundary, σ, using Krüss K10ST automated tensiometer. With this apparatus we only determine σ at fixed time after formation of the interface (not the kinetics). The time dependence of σ was explored using the recently developed "Fast Formed Drop" technique [8], which allows reliable measurements at times as short as ~50 ms. The principle of the method is to have a flow of surfactant solution through a glass capillary immersed in the oil, and to stop this flow suddenly by means of a stopcock. The drop remaining at the capillary tip is observed by a long focal distance microscope, images are taken, and the pressure is measured as a function of time. The output signal of the pressure transducer is amplified, fed to an Analogue-to-Digital Converter, and stored in a PC. The experimental details are fully described in Ref. [8].

**2.2.3. Interfacial dilatational rheology.** The elasticity and the (apparent) viscosity of an oil/water interface subjected to dilatational deformation are measured using the "Expanding Drop" technique [9]. It consists of forming a drop at the tip of a glass capillary, and expanding/compressing this drop by means of a syringe whose piston is connected to a DC-motor (Newport 860A). There is a piezoresistive pressure transducer (163PC01D36, Micro Switch), connected to the capillary. The syringe, the working part of the pressure transducer and the capillary are filled with soybean oil. The DC-motor provides a constant liquid flow, i.e., the change of the drop volume during the expansion is a linear function of time. The drop is observed by means of an optical microscope. Images are taken using a CCD video camera; they are recorded on a VCR and further processed by image analyser (grabbing board and the respective software). The electrical signal from the pressure transducer is amplified and stored in a computer through an analogue-digital converter (ADC).

The experimental procedure is as follows: After filling the system with the inner phase and reaching the desired temperature, we discard one drop and immediately form a fresh one. We wait for a certain period of time, $t_{\text{wait}}$, and then start the drop expansion squeezing the inner fluid out by means of the DC-motor. To achieve different stages of protein adsorption at the oil/water interface, four different times $t_{\text{wait}}$ were chosen: 20 s, 2 min, 5 min, and 15 min. In all experimental runs we performed controlled expansion with the following parameters: maximum total strain $\alpha_{\max} = 0.1$; estimated rate of strain $\dot{\alpha}_{\text{est}} = 0.025\ \text{s}^{-1}$. The relative dilatation, α, according to its definition, is $\alpha = \ln\left(A(t)/A_0\right)$, where $A(t)$ is the area of the drop surface at a moment $t$, and $A_0$ is the value of $A$ in the non-deformed state (at $t$=0, when the dilatation commences). $\alpha_{\max}$ is a measure for the final de-

viation of the adsorption layer from the initial state at $t$=0 in a given experimental run. The "estimated" rate of strain is in fact an average quantity over the time of expansion.

**2.2.4. Thin films in a porous glass cell (Mysels method).** We apply a technique similar to that proposed in Ref. [10]. A hole with diameter of about 2 mm is drilled in a plate of porous glass (with micron-size pores). This plate is sealed to a glass capillary which is filled with the investigated aqueous solution. The cell may be immersed in oil phase (if emulsion films are to be made), or in air (for foam films). The films are formed by sucking out the water phase, using a pressure control system with syringes whose pistons are pushed and pulled by micrometric screws. The capillary is connected to a transducer, so the pressure is measured directly. The films are observed in reflected monochromatic light (with wavelength $\lambda$=546 nm) by a microscope (Zeiss Axioplan), which gives us the interference picture with bright and dark areas. The instantaneous film thickness is determined from the intensity of the light, $I$, reflected from a small piece of area, according to the known formula

$$h = \frac{\lambda}{2\pi n_0}\left[k\pi \pm \arcsin\sqrt{\frac{I - I_{\min}}{I_{\max} - I_{\min}}}\right],$$

where $n_0$ is the refractive index of the film phase, $k$ is the order of the interference, and $I_{\min}$, $I_{\max}$ are the minimal and maximal values of the intensity $I$. Further details on the method can be found e.g. in Ref. [11].

**2.2.5. Film Trapping Technique (FTT).** This is a new method for studying the stability of emulsion droplets which are pressed in a liquid film on a solid substrate. All experimental details are described comprehensively in Ref. [12]. The principle of the technique is illustrated in Fig. 8c. A vertical glass capillary is held at a small distance apart from the flat bottom of a glass vessel. The lower capillary edge is immersed in the aqueous phase from which the wetting film is formed. The capillary is supported by positioning device with micrometric X, Y, Z translators and a tilting adjustment gadget. Thus one can approach the lower capillary forehead very closely to the glass bottom, in a position exactly parallel to the substrate. This setup is mounted on the stage of an inverted optical microscope (Carl Zeiss Jena, with objective Zeiss LD Epiplan 20×). The observation is carried out from below, through the substrate, in reflected monochromatic light ($\lambda$ = 546 nm), as well as in transmitted white light. In reflected light one sees an interference picture representing the topology of the Plateau borders around the drops. The capillary is connected to a pneumatic pressure control system. One can measure the difference between the pressure of air inside the capillary and the atmospheric pressure, using a sensor connected to the pressure control system. It is then straightforward to find the capillary pressure, $P_C$, across the liquid menis-

cus between the bulk oil and water phases- see Figs. 8b, c. The hydrostatic pressures are of course taken into account.

If the aqueous phase contains oil droplets, they can be trapped in the wetting film. To do this, we increase the pressure inside the capillary, and then the oil-water interface moves downward to the substrate. During this motion the interface pushes the oil drops which float in the water. When the distance between the oil/water interface and the glass substrate becomes equal to or smaller than the size of the drops, they remain entrapped in the oil-water-glass layer (Figs. 8b, c). In fact, one can use the meniscus approaching the substrate as a precise tweezers by which one can exert accurate and controllable capillary pressure on the sandwiched drops. $P_C$ acts as a pressing force, and we are interested especially in the critical value of $P_C$ (denoted by $P_C^{CR}$) when coalescence takes place.

## 3 STABILITY OF EMULSION DROPS

We measured the lifetime of large xylene drops whose radii were in the range 300-1400 μm (with the experiment described in Section 2.2.1). Basically, it turned out that part of the droplets lived for a very short time (seconds), but others survived for longer periods. No appreciable dependence on the size was noticed. On the other hand, the effect of the protein concentration was very well pronounced. Figure 1a shows the results for the fraction of drops whose lifetime exceeds 2 minutes (in a system with BLG). This fraction is found to increase considerably with rising protein content. It is also evident that when the o/w interface of the drops is pre-equilibrated the stability is better. Therefore, the data demonstrate that both the adsorption kinetics and the equilibrium adsorbed amount are important.

The average lifetime of the "long-living" drops (which survive for more than 2 min) in saturated systems, when aged emulsion is released to the large liquid surface, is plotted in Fig. 1b. The error bar at $10^{-3}$ wt% represents the typical scattering of the data: the confidence interval is ±119 s for the mean value 513 s from 10 independent measurements of drops with sizes 300-1400 μm (at 95% level of statistical certainty). Above $10^{-3}$ wt% BLG the droplets are infinitely stable, which means that no coalescence occurs for at least 30 minutes (in some cases we waited 90 min without ever observing rupture). The lifetime is compared with the time for thinning of the aqueous film formed between the (deformed) drop and the homophase. An example of such a film is presented in Fig. 2 (the picture was taken in reflected monochromatic light, so the interference pattern is seen). The films (at pH=6.2) thin down until the black portion occupies almost the whole area (the protein aggregates are gradually smashed). Afterwards, coalescence may take place. The time elapsed from the film formation until the moment when no further change in the film thickness is noticed is called tinning time, $\tau_t$. From Fig. 1b we see that at low concentrations (below

~$10^{-3}$ wt% BLG) the time for thinning is close to the lifetime. In other words, the films rupture soon after they reach their final thickness. In contrast, at higher concentrations stable equilibrium films are formed, and then the stability is not related to the thinning.

A question may arise as to whether the thinning rate, $V$, at low protein content is affected by interfacial mobility. The hydrodynamic theory states that [13]

$$\tau_t = \int_{h_f}^{h_{in}} \frac{dh}{V(h)} \; ; \qquad V(h) = -\frac{dh}{dt} = V_{\mathrm{Re}} \left(1 + \frac{h_s}{h}\right) , \tag{1}$$

where $\tau_t$ is the time for film thinning from the initial thickness $h_{in}$ to the final thickness $h_f$, $F$ is the driving force which pushes the film surfaces toward each other, and the "Reynolds velocity",

$$V_{\mathrm{Re}} = \frac{2h^3 F}{3\pi\eta r^4} , \tag{1a}$$

is the velocity of thinning of a film whose surfaces are immobile (this happens at high surfactant concentrations). In the above equations $\eta$ is the viscosity of the continuous phase, $r$ and $h$ are the film radius and thickness, and $h_s$ is a characteristic parameter, having dimension of thickness, which is a measure for the degree of interfacial mobility [13]:

$$h_s = 6\eta D_s / E_G \; . \tag{2}$$

Here $D_s$ is the surface diffusion coefficient of the adsorbed amphiphilic species, and $E_G$ is the Gibbs elasticity. The diffusion along the interface moves the surfactant opposite to the existing gradient of the surface pressure in the thinning film (accounted for by the Gibbs' elasticity, $E_G$), thus relaxing the surface stress and increasing the rate of thinning $V$ with respect to its value $V_{\mathrm{Re}}$ for tangentially immobile interfaces. This effect of the surface mobility is included in the term $h_s/h$ in Eq. (1).

Clark [14] has reported that $D_s$ = 1.5-3.5×$10^{-7}$ $cm^2/s$ in BLG layers, which is slightly lower than the bulk diffusion coefficient, $D$= 7.8×$10^{-7}$ $cm^2/s$. On the other hand, the lowest Gibbs' elasticity that we could measure for BLG was 2 dyn/cm (see Fig. 5). The dilatational elasticity of aged water/air interfaces covered by BLG was determined to be above 50 dyn/cm in Ref. [15], for bulk concentrations in the range $10^{-3}$-0.1 wt% (at $10^{-4}$ wt% the elasticity modulus is 53 dyn/cm). Thus, Eq. (2) (with $D_s \approx D$) gives $h_s < 0.3$ nm, which means that the film interfaces are completely immobile from the point of view of the hydrodynamics ($h_s << h$ in Eq. (1)). Such a conclusion is supported also by the observation that BLG forms an elastic gel-like network even at rather low concentrations (e.g., $10^{-3}$ wt% [15]).

Another effect frequently invoked in explaining emulsion stability is that of the surface viscosity. It has been studied theoretically in several papers (see e.g. [3], [4], [5], [13], [16]), but the theories are rather complicated and usually the final results are obtained in numerical form. It is not difficult however to reach the main conclusions by a simple estimate. The surfactant mass balance on the interface is determined by two main effects: surface convection and diffusion (the effect of the bulk diffusivity is negligible):

$$\underbrace{\Gamma\left(\frac{\partial v_x}{\partial x}\right)}_{Convection} = \underbrace{D_s\left(\frac{\partial^2 \Gamma}{\partial x^2}\right)}_{Surface\ diffusion} \quad . \tag{3}$$

Here $x$ is the coordinate along the film surface and $v_x$ is the respective component of the fluid velocity; $\sigma$ and $\Gamma$ are the local values of the interfacial tension and adsorption. Since the film radius $r$ is the natural scale in $x$–direction, one can substitute the term $\partial^2\Gamma/\partial x^2$ according to the approximate relation $(\partial\Gamma/\partial x) \propto r(\partial^2\Gamma/\partial x^2)$. With this expression and with Eq. (3), one can write the ratio of the surface viscous stress to the surface elastic stress in the form (cf. also Eq. (2)):

$$\frac{Viscous\ stress}{Elastic\ stress} \propto \frac{\eta_s(\partial^2 v_x/\partial x^2)}{(\partial\sigma/\partial\Gamma)(\partial\Gamma/\partial x)} \propto \frac{\eta_s D_s}{r^2 E_G} \propto \frac{\eta_s h_s}{\eta r^2} . \tag{4}$$

The most important conclusion stemming from this result is that the effect of the surface viscosity is always coupled with the surface mobility through $h_s$ – if there is enough surfactant to render the interface immobile, i.e. to decrease $h_s$ to zero, then the surface viscosity, no matter how large, will play no role. And we saw already that $h_s$ is very small for protein containing systems. The effect of the surface viscosity is additionally decreased by the presence of the factor $r^2$ in the denominator–even for the very low protein concentrations considered here, for which $h_s$ does not exceed 0.3 nm, the above ratio will become unity (i.e., the elastic and viscous stresses will become equally important) only if the surface viscosity becomes ~0.3 sp (for film radii 10 μm). Let us keep in mind that $\eta_s$ is the *true* surface viscosity, i.e. the one which is determined only by the interactions between the adsorbed molecules, because the theory which leads to Eq. (1) accounts for the apparent surface viscosity by considering separately the surfactant diffusion. Such relatively high true surface viscosities can be observed only in concentrated adsorbed layers, but then the Gibbs' elasticity will be also very high and $h_s$ will be even smaller, thus compensating the increase of $\eta_s$. Hence,

we are left with the conclusion that, at least as far as film thinning is concerned, the surface viscosity will play negligible role for any realistic values of the system parameters.

In the limit of immobile surfaces the thinning velocity $V$ reduces to $V_{\mathrm{Re}}$ (Eq. (1a)), whence

$$\tau_t = \frac{3\pi\eta r^4}{4F h_f^2} = \frac{\eta\Delta\rho g}{h_f^2}\frac{R^5}{\sigma^2} \ . \qquad (5)$$

The last equality in (5) holds if $F$ is due to buoyancy; the film radius $r$ was expressed in terms of the drop radius, $R$, and the interfacial tension, $\sigma$, through the formula $r^2 = F R/(\pi\sigma)$ - Ref. [13]. In diluted systems the final film thickness, $h_{\mathrm{f}}$, in fact coincides with the critical thickness for rupture, $h_{\mathrm{cr}}$. The latter quantity has been calculated theoretically [17], and the results agree well with experimental measurements. As a rule, $h_{\mathrm{cr}}$ tends to increase with diminishing concentration of surfactant, but the effect is not large. Especially with a globular protein (BSA), there is virtually no dependence of $h_{\mathrm{cr}}$ on the protein content whatsoever [17].

Let us now estimate $h_{\mathrm{f}}$ from the data in Fig. 1b. The thinning time was measured only for films made by drops with $R$≈300 μm. At $8\times10^{-4}$ wt% BLG the interfacial tension of the water/xylene boundary was determined to be 19 dyn/cm (cf. Fig. 3); $\Delta\rho$= 0.12 g/cm$^3$, and with $\tau_{\mathrm{t}}$ = 120 s Eq. (5) yields $h_{\mathrm{f}}$≈ 8.1 nm. This value seems to be reasonable if the final state of the film is close to a bilayer, since the thickness of the adsorbed monolayer of BLG (measured by neutron reflectivity) is of the order of 3.5-4 nm [18]. Besides, the estimate for $h_{\mathrm{f}}$ is corroborated (as an order of magnitude) by thickness measurements in Mysels cell- see below. We arrive at the conclusion that at low concentrations (between 3 and $8\times10^{-4}$ wt% BLG) the thinning basically follows the Reynolds law for tangentially immobile interfaces.

Figure 1b shows that for concentrations above ~$8\times10^{-4}$ - $10^{-3}$ wt% the thinning time increases considerably, and the lifetime goes to infinity. There are two possible reasons for the slower thinning: (i) increased number of lumps in the films- see Fig. 2, whence the draining liquid has to overcome greater hydrodynamic resistance, and the squashing of the aggregates is more difficult; (ii) development of stronger repulsive interactions between the protein-laden film surfaces. The latter repulsion may also be responsible for the high stability against rupture- evidence for this will be provided below.

Let us now explore the reasons for the stability trends illustrated in Fig. 1. It is natural to think of continuously increasing adsorption, and rate of adsorption, as the bulk concentration rises. So far in the literature there are scarce data for the adsorbed amount ($\Gamma$) of BLG on liquid interfaces as a function of the concentration ($c$). Miller et al. [19] reported

that Γ first increases with *c*, and then reaches a more or less constant value of about 1.6-1.8 mg/m$^2$ after *c*~ 2×10$^{-4}$ wt% BLG (up to ~0.02 wt%). Those results were obtained by ellipsometry on air/water interface. Atkinson et al. [18] carried out neutron reflectivity on A/W surface and found that Γ= 1.64 mg/m$^2$ for 10$^{-3}$ and 10$^{-2}$ wt% BLG. Cornec et al. [20] applied radiotracer technique, and observed that the rate of adsorption increased substantially with *c* in the interval 5×10$^{-5}$ - 2×10$^{-4}$ wt% BLG.

Indirect information about the adsorption and the lateral interactions within the surface can be gained from the changes of the interfacial tension, σ. Kraegel et al. [21] studied a wide range of BLG concentrations. From 1.8×10$^{-5}$ to 0.18 wt% σ at the air/water boundary (aged for 1, 3 and 24 hours) was found to decrease continuously as a function of *c*. Results from our own measurements on xylene/water surface (at one hour after formation) are shown in Fig. 3. One notices that at concentrations above 10$^{-3}$ wt% there is only a relatively slight change of σ as a function of log(*c*), which may be an indication for saturation of the interfacial layer- compare with the infinite stability of the drops in Fig. 1b. Regarding the kinetics, the data of Ref. [21] (Fig. 2 therein) for a/w boundary confirm that the higher the bulk concentration the faster the adsorption (in a time scale of minutes). Our measurements with a fast-formed aqueous drop in soybean oil permitted studying shorter times- of the order of seconds. Figure 4 contains results for four concentrations of BLG. Evidently, with more protein in the bulk the adsorption rate is higher. This is perhaps not surprising, because it is now an established fact that the initial stage of protein adsorption is diffusion-controlled [20]. Then, the short-time asymptote of Γ predicts that $\Gamma = 2c\sqrt{Dt/\pi}$ .

To summarise, we wish to point out that at higher protein concentrations saturation of the interface is reached faster. This brings about increased stability- Fig. 1. After ~10$^{-3}$ wt% BLG the adsorption at short times becomes sufficient to stabilise non-equilibrated systems (Fig. 1a), and the drops in aged systems exhibit infinite lifetime (Fig. 1b).

Let us now consider the interfacial rheological properties of BLG layers. We applied the Expanding Drop method to measure the elasticity, *E*, and the (apparent) viscosity, $\eta_d$, of protein-laden o/w surfaces subjected to pure dilatation. The two quantities *E*, $\eta_d$ were obtained from the fit of the time dependence of the total stress, τ(*t*), according to Maxwell's rheological model (elastic and viscous elements connected in series):

$$\tau = \eta_d \, \dot{\alpha}_{mean} \left[ 1 - \exp\left( -\frac{E}{\eta_d} t \right) \right] . \qquad (6)$$

Here $\dot{\alpha}_{mean}$ denotes the average rate of drop expansion. Figure 5 shows data for $E$ as a function of the bulk concentration, $c$, at different times after formation of a new drop on the capillary tip. The trends in the experimental results are clearly discerned: with rising $c$ and with longer ageing the elasticity increases gradually. The dependence of $E$ on the ageing time is strong only at the smallest value of $t_{wait}$ - 20 sec. The surface viscosity, $\eta_d$, is greatly affected by mass exchange of protein with the bulk. As was discussed in Refs. [3], [22], the diffusion transfer of surfactant from the bulk towards the interface provides a significant contribution to $\eta_d$. That is why we will not present data for $\eta_d$ here.

Our findings for the elasticity are in consonance with the already discussed adsorption behaviour of BLG. In a time scale of ~15 minutes new amounts of protein still continue to adsorb, and therefore, the ageing should be accompanied with increasing $E$. On the other hand, effects of mechanical reinforcement of the layer may also exist (due to entanglement of neighbouring molecules and formation of a gel-like network)- let us recall that the equilibrium value of $\Gamma(c)$ does not change much at higher concentrations, but $\sigma(c)$ decreases continuously ([21], see above). The higher adsorption rates at rising $c$ can be responsible for the greater values of the parameter $E$, determined under the conditions of fixed time and increasing $c$. All these effects may favour the stability of emulsion droplets.

Another important factor, which is sometimes very efficient in preventing drop coalescence, is the repulsive interaction between the film surfaces. We measured the disjoining pressure, $\Pi$, as a function of the film thickness, $h$, in a porous glass cell (Mysels method). This gives us quantitative information about the magnitude of the repulsion and the threshold value of the pressing force when rupture occurs. The result for the $\Pi(h)$ isotherm in a foam film stabilised by 0.02 wt% BLG is shown in Fig. 6. First of all, we have to emphasize that the repulsion ($\Pi>0$) does not originate from electrostatic interactions. This is so because (i) it is impossible to fit the curve in Fig. 6 with a reasonable value of the Debye length, and (ii) because a similar isotherm has been obtained at the isoelectric point (pH=5.2), when the interfaces are not charged. Most probably, an osmotic effect due to partial overlapping of the opposing protein layers and/or steric repulsion (which might stem from existing small lumps) is responsible for the observed $\Pi(h)$ curve. In the system from Fig. 6 the critical pressure for rupture, $\Pi^{CR}=P_C{}^{CR}$, is about 2200 dyn/cm$^2$.

Let us pay attention to the final film thickness of about 12.2 nm. Knowing that the adsorbed monolayers of BLG have thickness of at most ~4 nm [18], we may suppose presence of some excess protein inside the film (in the form of small lumps), possibly mixed with water, or even a layer of water (stabilised by osmotic effects due to dangling protein tails, or by electrostatic repulsion- at this salt concentration the Debye length is ~0.8 nm).

Still, one has to be cautious with such hypotheses because the film thickness measurements by interferometry are not precise, especially in the range below ~30 nm. An error of ±3-4 nm is fully feasible with this method.

In order to be able to relate the data measured in films with the stability of emulsion droplets, we have undertaken a more extensive investigation on the conditions for coalescence of oil drops trapped in an aqueous film which is formed between a glass substrate and a large oil phase. The Film Trapping Technique is used for this purpose- see Fig. 7c. We measure the critical capillary pressure of the oil/water meniscus, $P_C^{CR}$ (Figs. 7b, c), when the intervening oil/water/oil film on the drop ruptures. The data for $P_C^{CR}$ are listed in Table 1: the protein concentration $c$ was varied from $5\times10^{-4}$ to $8\times10^{-3}$ wt% BLG, and the entrapped drops had radii ~10 μm. Due to experimental difficulties, larger drops could not be caught in the film. From Table 1 one sees that there is a systematic increase of $P_C^{CR}$ as $c$ rises, which is an indication for improved stability. A question now arises of how to connect the values of $P_C^{CR}$ determined in the configuration of Fig. 7b with the critical disjoining pressure for coalescence of a much larger oil drop pressed by buoyancy toward a large homophase- Fig. 7a (in the latter case $P_C = 0$). Figure 7a corresponds to the system geometry in our experiments when oil droplets (with radii $R\approx330$ μm) are released from a capillary beneath a flat o/w interface.

Bearing in mind that the disjoining pressure, according to its definition, is the pressure in the intervening oil/water/oil film minus the pressure $P_L$ in the water phase surrounding the drop (Figs. 7a, b), we may write the balances of the capillary pressures across the liquid menisci. It is straightforward to obtain the following relations, which hold in mechanical equilibrium:

$$\Pi_{drop} = \frac{\sigma}{R} \quad \text{for a spherical drop pressed to a free interface, Fig. 7a;} \tag{7}$$

$$\Pi = \frac{P_C}{2} + \frac{\sigma}{R} \quad \text{for a spherical drop trapped in a film on a plane substrate, Fig. 7b.} \tag{8}$$

$\Pi_{drop}$ and $\Pi$ are the disjoining pressures in the systems depicted in Figs. 7a and b, respectively; $R$ is the drop radius, $\sigma$ is the o/w interfacial tension, and $P_C$ is the capillary pressure of the large film in the FTT- Figs. 7b, c. Equation (8) can be written also for the "critical" conditions, when the drop coalesces under the pressing action of $P_C^{CR}$:

$$\Pi^{CR} = \frac{P_C^{CR}}{2} + \frac{\sigma}{R} \ . \tag{9}$$

Obviously, there are two contributions in $\Pi^{CR}$: one from $\sigma$ and the drop curvature ($\sigma/R$, which is equal to $\Pi_{drop}$), and another one, $P_C^{CR}/2$, that is the excess pressure of the o/w

meniscus necessary to provoke rupture. Now, the equations (7), (9) can be utilised to recalculate what the critical disjoining pressure $\Pi^{CR}$ would have been if relatively large drops ($R$≈330 μm) had been trapped and forced to coalesce between the o/w meniscus and the substrate in the FTT (Figs. 7b, c). We take the respective value of σ from Fig. 3, divide by $R$= 330 μm, and add $P_C^{CR}/2$ from Table 1. Our observations have shown that $P_C^{CR}$ does not depend on the drop radius, so we suppose $P_C^{CR}$ is the same for $R$~10 μm and $R$~330 μm. The results are plotted in Fig. 8. $\Pi^{CR}$ at the point for 0.02 wt% BLG was calculated with $P_C^{CR}$ = 2200 dyn/cm$^2$, measured in the Mysels cell- Fig. 6.

In Fig. 8 the values of $\Pi^{CR}$ are compared with $\Pi_{drop}$, the latter referring to mechanical equilibrium in the configuration of Fig. 7a (without excess pressing force). $\Pi_{drop}$ (the full circles in Fig. 8) corresponds to real drops released to o/w boundary in our experiments from Section 2.2.1. What we see is that at concentrations below ~$10^{-3}$ wt% BLG $P_C^{CR}/2$ is negligible with respect to σ/$R$, and therefore, $\Pi^{CR} \approx \Pi_{drop}$. In other words, as soon as the drop comes to the o/w interface and mechanical equilibrium with $\Pi=\Pi_{drop}$ is established in the experiment depicted in Fig. 7a, the drop should coalesce. This is exactly what is observed in reality- see Fig. 1b. We have already noted that at low concentrations the coalescence happens almost immediately after the film thinning is completed. In contrast, at higher protein concentrations $\Pi^{CR} > \Pi_{drop}$ (Fig. 8), and the drops are not supposed to rupture (because they stay at $\Pi_{drop}$ and there is no excess pressing force in the configuration of Fig. 7a). From Fig. 1b it is seen that the lifetime indeed goes to infinity. As a matter of fact, certain fraction of drops do coalesce (Fig. 1a). This could be attributed to the statistical nature of the process of film rupture. Perhaps, the probability for rupture is correlated with the difference between $\Pi^{CR}$ and $\Pi_{drop}$.

We are now able to conclude that repulsive interactions between the two film surfaces (Fig. 6) determine the threshold force necessary for rupture and drop coalescence. At concentrations of BLG above ~$10^{-3}$ wt% the repulsion is sufficiently high, so that the buoyancy force acting on the drop cannot bring about rupture when the drop just stays at a large homophase. The drops remain stable if no excess pressing force is exerted on them.

A final remark will be concerned with the role of the electrostatic interactions for the drop stability. We performed some experiments at the isoelectric point of BLG (pH=5.2), and the data are shown in Fig. 1. Interestingly, there is no significant difference between the fractions of surviving drops in the cases of pH=6.2 and pH=5.2. This indicates that the repulsion mentioned above is not due to electrostatics (since at pH=5.2 the protein-laden liquid boundary is not charged). Other sources of repulsion (osmotic and/or steric interactions associated with partial overlapping of the opposing protein layers) may be relevant in our

systems. It is difficult to explain the differences in the stability at $1\times10^{-3}$ wt% BLG for pH=6.2 and 5.2- Fig. 1b. It is likely that the protein conformation, which is known to be sensitive to pH, influences the stiffness of the layers and their resistance to rupture.

## 4 CONCLUSIONS

We have demonstrated that the stability of emulsion drops pressed by buoyancy against a large homophase increases with the concentration of a globular protein (BLG) in the aqueous continuous phase. Repulsive interactions (other than electrostatics) prevent rupture of the intervening o/w/o films above a protein content of about $10^{-3}$ wt%. Then, the threshold disjoining pressure for coalescence is higher than the equilibrium disjoining pressure, and this correlates with very long lifetimes of drops. Conversely, at low concentrations the films rupture soon after the process of thinning is completed (the thinning time agrees with simple estimates based on the Reynolds formula for tangentially immobile interfaces).

Faster formation of saturated adsorption layers is probably responsible for the more efficient stabilisation at elevated concentrations. The adsorption kinetics in the time scales of seconds and minutes is rather sensitive to the protein content. Interfacial rheological measurements give evidence that with increasing concentration of protein the layer is mechanically reinforced to some extent.

## 5 ACKNOWLEDGEMENTS

This work was supported in part by Kraft Foods, Inc., USA, and in part by Inco-Copernicus project No. IC15 CT98 0911 of the European Commission. The authors I.I. and T.G. also wish to thank the Organising Committee of the Conference Food Colloids 2000 for providing financial assistance to their participation.

## REFERENCES

1 P. Walstra and P.E.A. Smulders, *Emulsion Formation*, in: "Modern Aspects of Emulsion Science" (B.P. Binks, Ed.), Royal Soc. Chemistry, Cambridge, 1998, Chapter 2, p. 56.

2 V. Schröder and H. Schubert, in: "Food Emulsions and Foams. Interfaces, Interactions and Stability" (E. Dickinson and J.M. Rodriguez Patino, Eds.), Royal Soc. Chemistry, Cambridge, 1999, pp. 70-80; V. Schröder, O. Behrend and H. Schubert, J. Colloid Interface Sci., 1998, 202, 334-340.

3 I.B. Ivanov and D.S. Dimitrov, *Thin Film Drainage*, in: "Thin Liquid Films" (I.B. Ivanov, Ed.), Marcel Dekker, New York, 1988, Chapter 7, p. 379.

4 D.A. Edwards, H. Brenner and D.T. Wasan, "Interfacial Transport Processes and Rheology", Butterworth-Heinemann, Boston, 1991.

5 I.B. Ivanov and D.S. Dimitrov, Colloid & Polymer Sci., 1974, 252, 982-990.
6 J.N. Israelachvili, "Intermolecular and Surface Forces", Academic Press, London, 1992.
7 E.S. Basheva, T.D. Gurkov, I.B. Ivanov, G.B. Bantchev, B. Campbell and R.P. Borwankar, Langmuir, 1999, 15(20), 6764-6769.
8 T.S. Horozov and L.N. Arnaudov, J. Colloid Interface Sci., 1999, 219, 99.
9 T.S. Horozov, K.D. Danov, P.A. Kralchevsky, I.B. Ivanov and R.P. Borwankar, Proceedings of the First World Congress on Emulsion, October 19-22, 1993, Paris, France, Volume 2, Contribution # 3-20.137; T.S. Horozov, P.A. Kralchevsky, K.D. Danov and I.B. Ivanov, J. Dispersion Sci. Technol., 1997, 18(6&7), 593-607.
10 K.J. Mysels and M.N. Jones, J. Phys. Chem., 1964, 68, 3441; Disc. Faraday Soc., 1966, 42, 42-50.
11 A. Scheludko and D. Exerowa, Kolloid Zeitschrift, 1959, 165, 148; T.T. Traykov, E.D. Manev and I.B. Ivanov, Int. J. Multiphase Flow, 1977, 3, 485-494.
12 A.D. Hadjiiski, S.C. Tcholakova, I.B. Ivanov, T.D. Gurkov and E. Leonard, "Gentle Film Trapping Technique with Application to Drop Entry Measurements", Langmuir, 2000, submitted.
13 I.B. Ivanov, Pure & Appl. Chem., 1980, 52, 1241-1262.
14 D.C. Clark, in: "Characterization of Food: Emerging Methods" (A.G. Gaonkar, Ed.), Elsevier, Amsterdam, 1995, Chapter 2, p. 23.
15 J.T. Petkov, T.D. Gurkov, B. Campbell and R.P. Borwankar, Langmuir, 2000, 16(8), 3703-3711.
16 D.E. Tambe and M.M. Sharma, J. Colloid Interface Sci., 1991, 147(1), 137-151.
17 D.S. Valkovska, K.D. Danov and I.B. Ivanov, "Effect of surfactants on the stability of films between two colliding small bubbles", Colloids Surfaces A, 2000, in press.
18 P.J. Atkinson, E. Dickinson, D.S. Horne and R.M. Richardson, J. Chem. Soc. Faraday Trans., 1995, 91(17), 2847-2854.
19 R. Miller, V.B. Fainerman, A.V. Makievski, D.O. Grigoriev, P. Wilde and J. Kraegel, in: "Food Emulsions and Foams. Interfaces, Interactions and Stability" (E. Dickinson and J.M. Rodriguez Patino, Eds.), Royal Soc. Chemistry, Cambridge, 1999, pp. 207-222.
20 M. Cornec, D. Cho and G. Narsimhan, J. Colloid Interface Sci., 1999, 214, 129-142.
21 J. Krägel, R. Wüstneck, D. Clark, P. Wilde and R. Miller, Colloids Surfaces A, 1995, 98, 127-135.
22 V.G. Levich, *Physicochemical Hydrodynamics*, Prentice-Hall, Englewood Cliffs, N.J., 1962.

## FIGURE CAPTIONS

**Figure 1.** (a) Fraction of droplets living for more than 2 minutes after they have been released towards a large oil/water interface (experiment 2.2.1, Section 2). (b) Thinning time and lifetime of the long-living drops from case (a). The thinning time refers to drops with radius $R \approx 300$ μm only.

**Figure 2.** Aqueous film of emulsion type, formed by a drop of xylene pressed by buoyancy to a large homophase. The system is stabilised with $3\times10^{-4}$ wt% BLG in the presence of 0.15 M NaCl+0.1 g/l $NaN_3$, pH=6.2 (natural). The reference distance between the bars is equal to 20 μm.

**Figure 3.** Interfacial tension of the flat xylene/water boundary, plotted as a function of the protein concentration (BLG). The measurements were performed by du Nouy platinum ring method, 1 hour after formation of the surface.

**Figure 4.** Kinetics of time changes of the soybean oil/water interfacial tension in the presence of BLG (+0.15 M NaCl+0.1 g/l $NaN_3$, pH=6.2). The protein concentrations are indicated on the curves. The Fast Formed Drop technique [8] was used for the measurements.

**Figure 5.** Elasticity $E$ of the soybean oil/water interface, extracted from fits of the time evolution of the stress according to the Maxwell rheological model (Eq. (6)). The Expanding Drop method was used for the measurements. The four curves correspond to different waiting times from the moment of drop formation until the start of dilatation.

**Figure 6.** Disjoining pressure isotherm, $\Pi(h)$, for a foam film studied in a Mysels porous glass cell. The film did not contain protein lumps. The thickness was measured interferometrically.

**Figure 7.** (a) Sketch of a drop pressed by buoyancy against a free flat o/w interface (this case corresponds to the experiment 2.2.1, Section 2). (b) Sketch of a drop entrapped in a wetting aqueous film on a substrate. $P_C$ is the capillary pressure of the oil/water meniscus. (c) Sketch of the system in the Film Trapping Technique.

**Figure 8.** Equilibrium disjoining pressure, $\Pi_{drop}$, of films made by drops pressed by buoyancy against a free flat o/w interface (full circles, Eq. (7)), and the critical disjoining pressure for rupture, $\Pi^{CR}$, if the drops had been entrapped in a wetting aqueous film on a substrate (open triangles and the plus symbol, Eq. (9)).

**Table 1.** Critical pressures for drop coalescence, measured by means of the Film Trapping Technique (FTT). The system is of emulsion type (oil/water/oil) and contains BLG at the natural pH (6.2), 0.15 M NaCl and 0.1 g/l $NaN_3$. The hydrophobic phase is soybean oil; the radius of the trapped drops is ~10 μm.

| $c_{BLG}$, wt% | $5\times10^{-4}$ | $6\times10^{-4}$ | $8\times10^{-4}$ | $1\times10^{-3}$ | $3\times10^{-3}$ | $8\times10^{-3}$ | $2\times10^{-2}$ |
|---|---|---|---|---|---|---|---|
| $P_C^{CR}$, dyn/cm$^2$ | 100 | 150 | 170 | 230 | 320 | 930 | 2200* |

*This value was obtained in a porous glass cell (Mysels method).

**(a)**

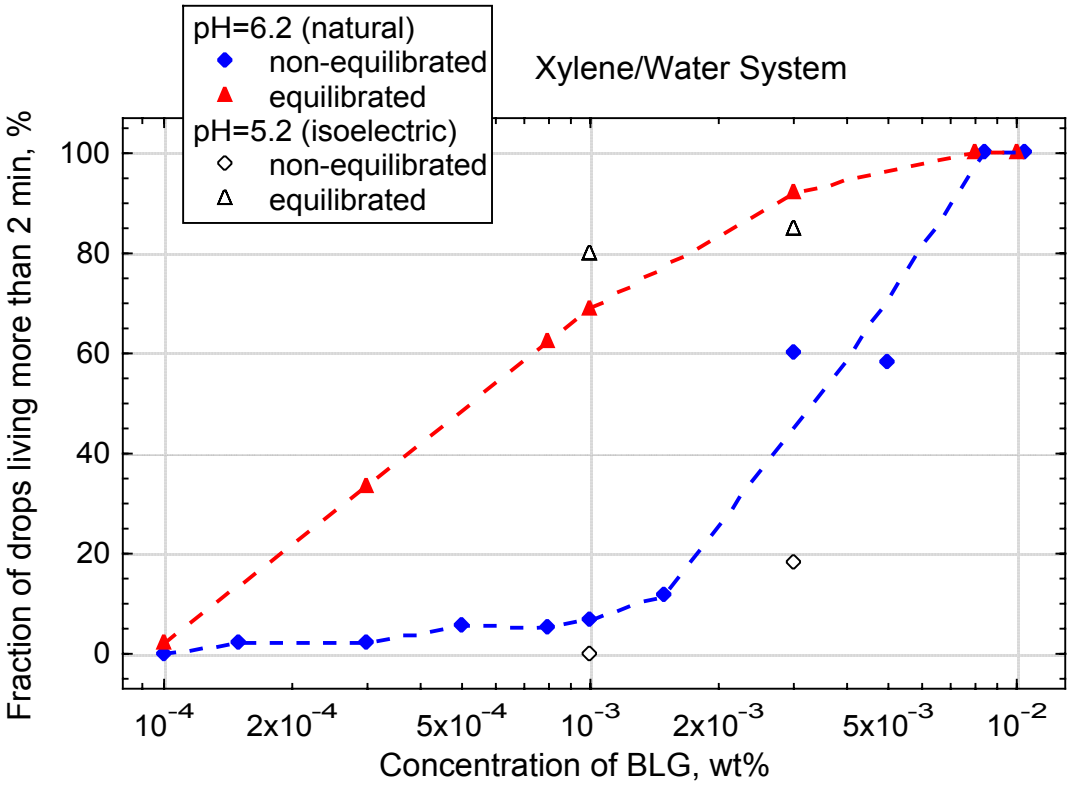


**(b)**

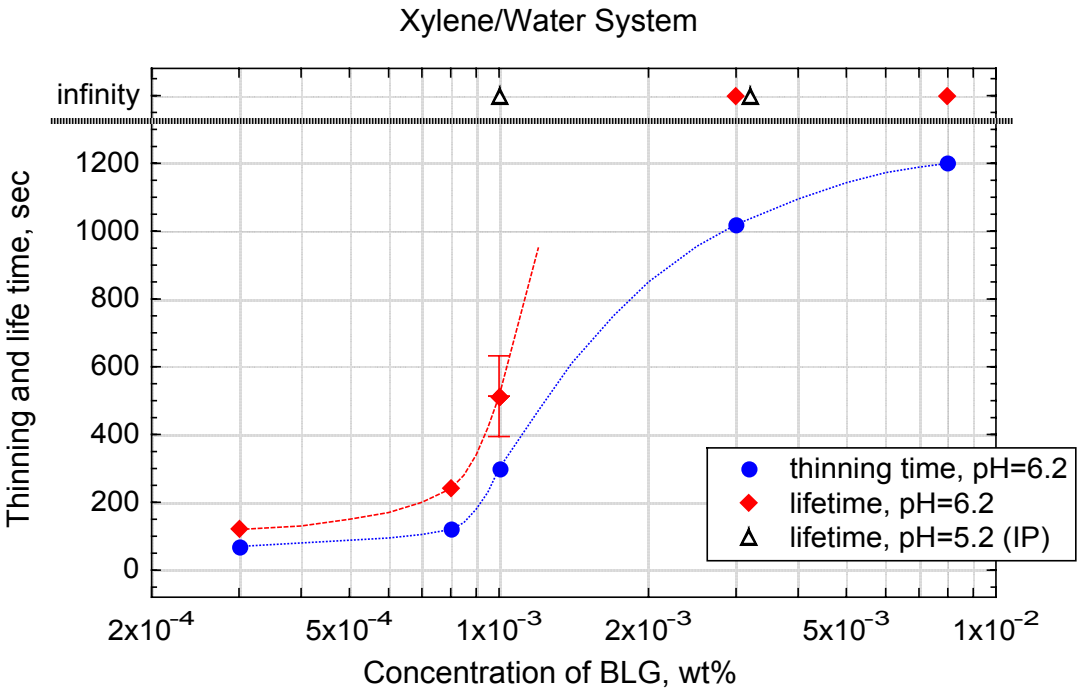


**Figure 1.** (a) Fraction of droplets living for more than 2 minutes after they have been released towards a large oil/water interface (experiment 2.2.1, Section 2). (b) Thinning time and lifetime of the long-living drops from case (a). The thinning time refers to drops with radius $R \approx 300$ μm only.

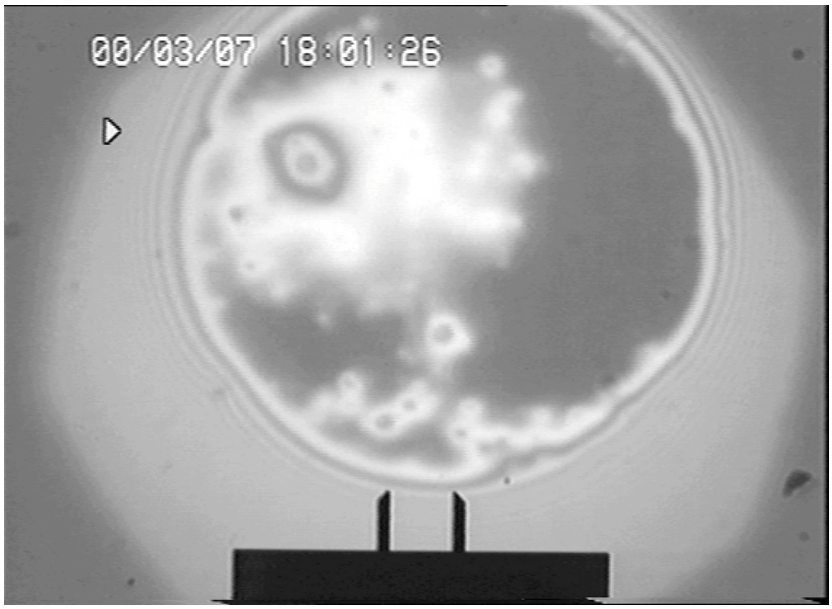


**Figure 2.** Aqueous film of emulsion type, formed by a drop of xylene pressed by buoyancy to a large homophase. The system is stabilised with $3\times10^{-4}$ wt% BLG in the presence of 0.15 M NaCl+0.1 g/l $NaN_3$, pH=6.2 (natural). The reference distance between the bars is equal to 20 μm.

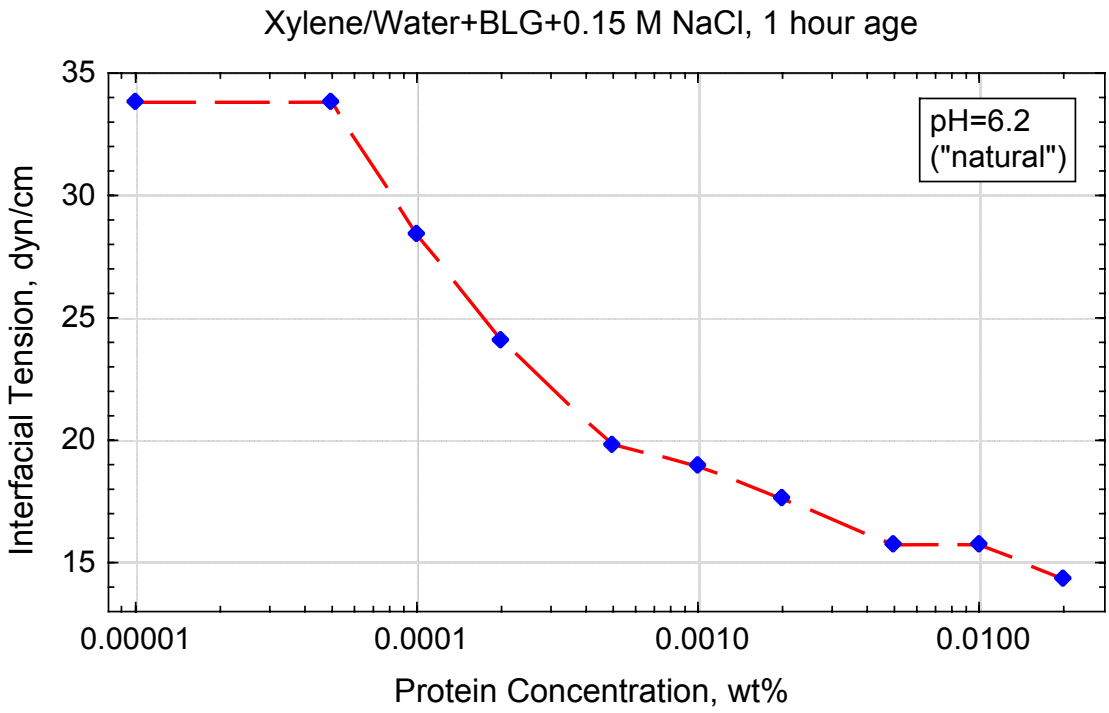


**Figure 3.** Interfacial tension of the flat xylene/water boundary, plotted as a function of the protein concentration (BLG). The measurements were performed by du Nouy platinum ring method, 1 hour after formation of the surface.

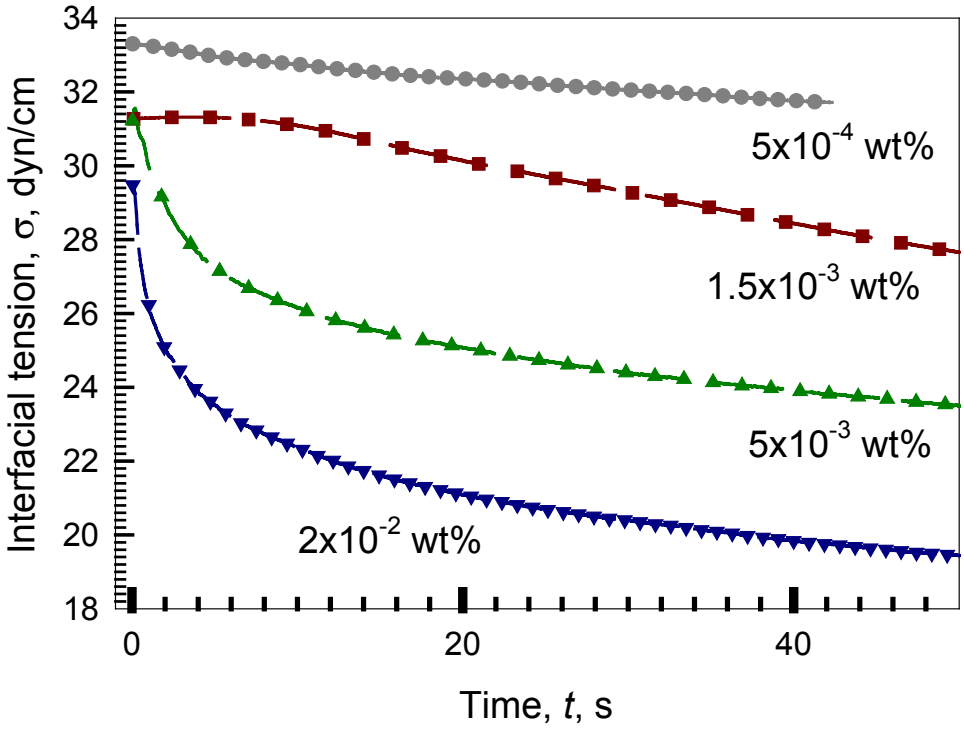


**Figure 4.** Kinetics of time changes of the soybean oil/water interfacial tension in the presence of BLG (+0.15 M NaCl+0.1 g/l $NaN_3$, pH=6.2). The protein concentrations are indicated on the curves. The Fast Formed Drop technique [8] was used for the measurements.

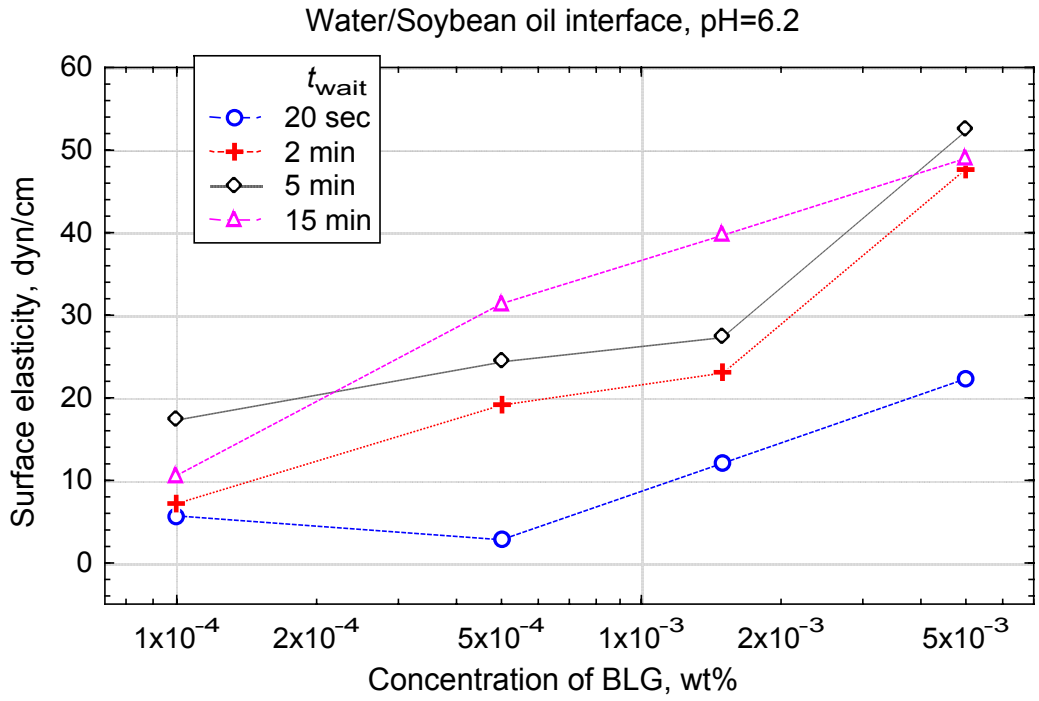


**Figure 5.** Elasticity $E$ of the soybean oil/water interface, extracted from fits of the time evolution of the stress according to the Maxwell rheological model (Eq. (6)). The Expanding Drop method was used for the measurements. The four curves correspond to different waiting times from the moment of drop formation until the start of dilatation.

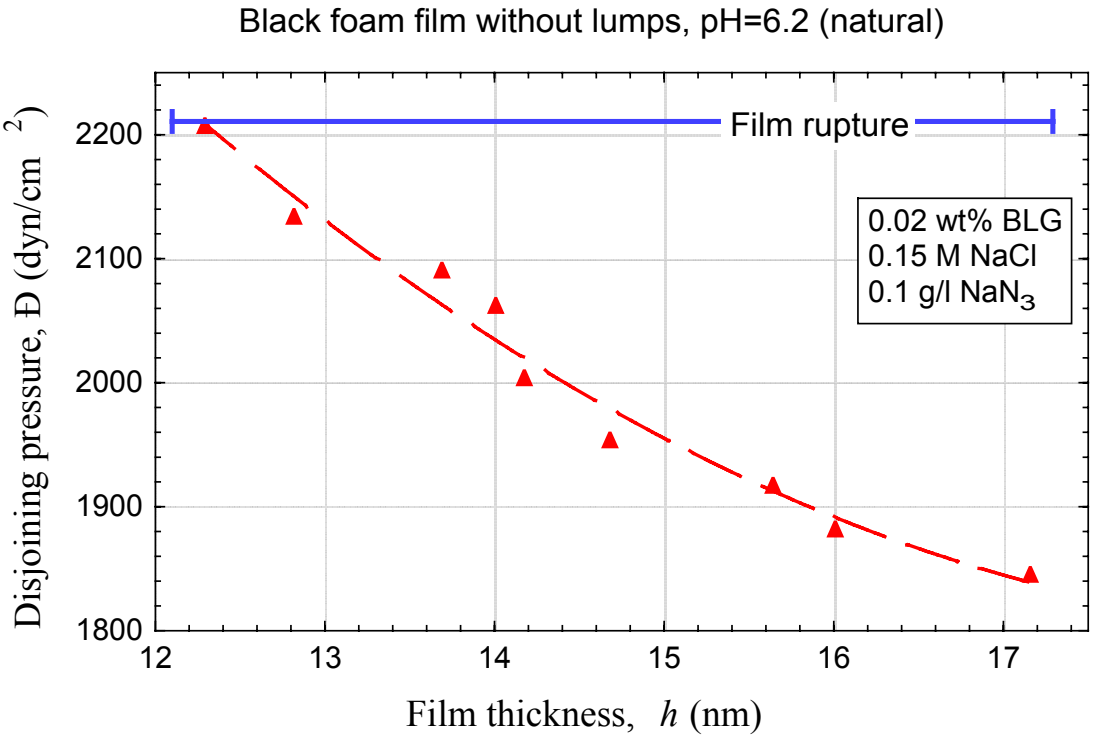


**Figure 6.** Disjoining pressure isotherm, $\Pi(h)$, for a foam film studied in a Mysels porous glass cell. The film did not contain protein lumps. The thickness was measured interferometrically.

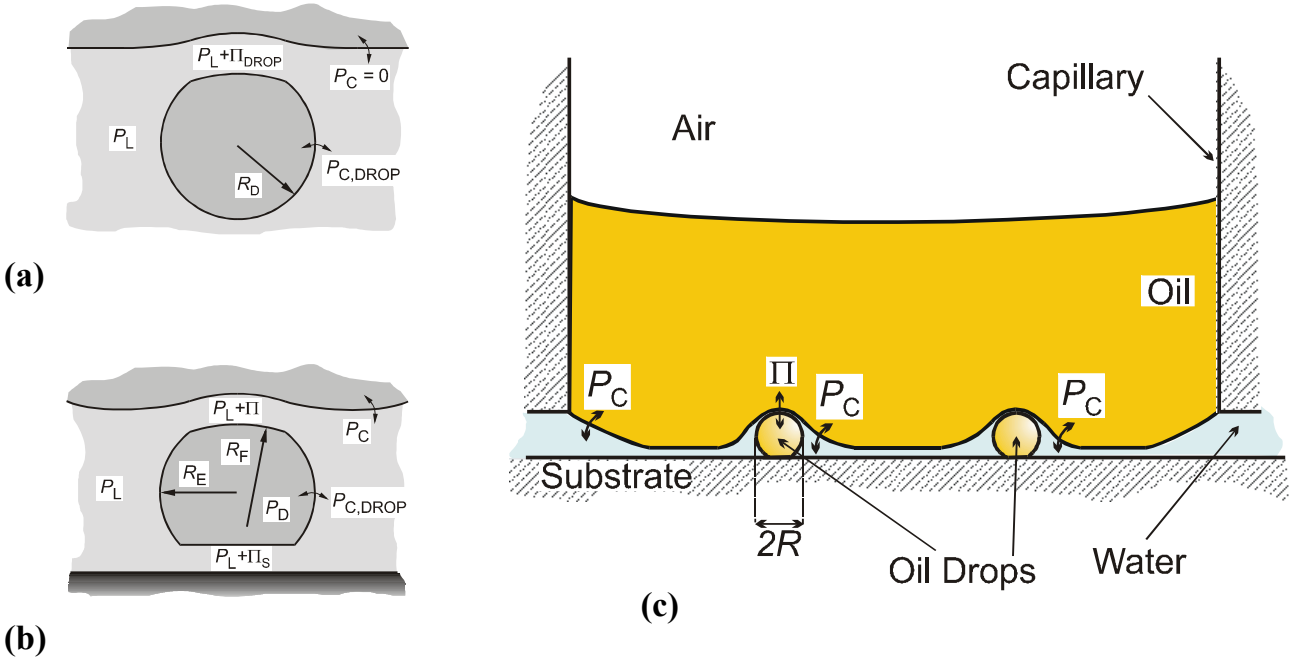


**Figure 7.** (a) Sketch of a drop pressed by buoyancy against a free flat o/w interface (this case corresponds to the experiment 2.2.1, Section 2). (b) Sketch of a drop entrapped in a wetting aqueous film on a substrate. $P_C$ is the capillary pressure of the oil/water meniscus. (c) Sketch of the system in the Film Trapping Technique.

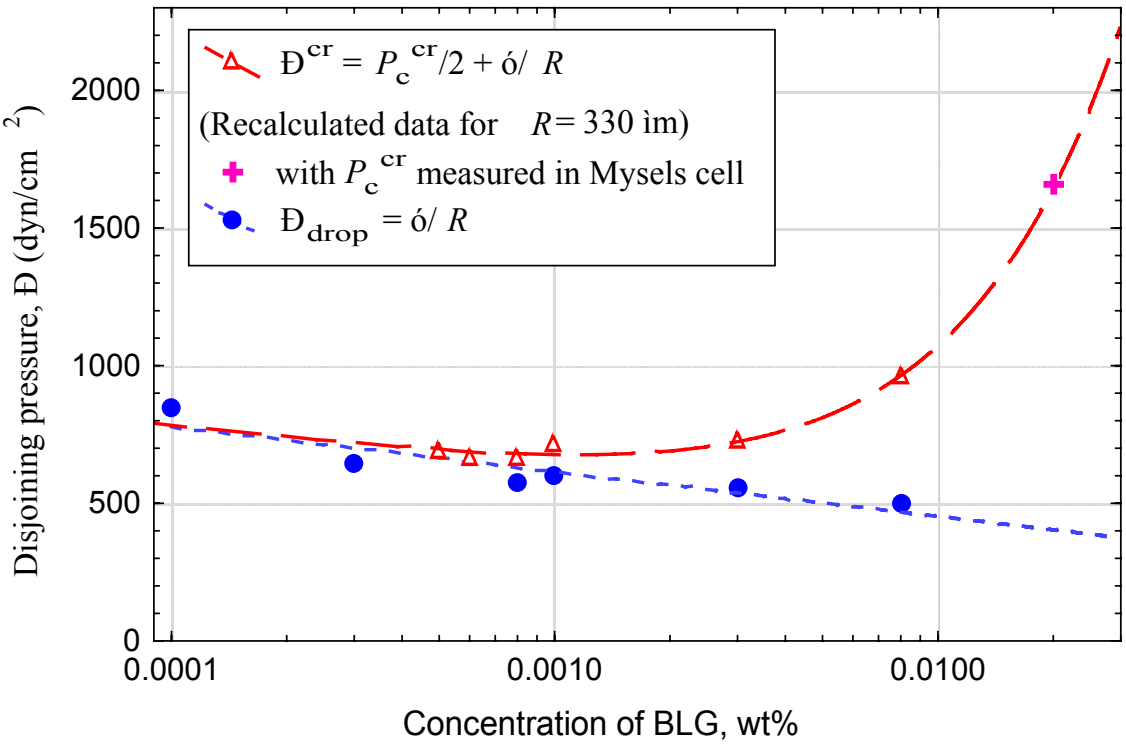


**Figure 8.** Equilibrium disjoining pressure, $\Pi_{drop}$, of films made by drops pressed by buoyancy against a free flat o/w interface (full circles, Eq. (7)), and the critical disjoining pressure for rupture, $\Pi^{CR}$, if the drops had been entrapped in a wetting aqueous film on a substrate (open triangles and the plus symbol, Eq. (9)).